Applied Nanoscience (2020) 10:3925–3931
https://doi.org/10.1007/s13204-020-01476-x

ORIGINAL ARTICLE

Visible light responsive photocatalytic hydrogen evolution using MoS2 incorporated ZnO

Muhammad Bilal Tahir[1] · Muhammad Sohaib[1] · Muhammad Rafique[2] · Muhammad Sagir[3] · Najeeb Ur Rehman[4] · Shabbir Muhammad[5,6]

Received: 14 May 2020 / Accepted: 3 June 2020 / Published online: 9 June 2020

Abstract
In this article, we prepared efficient ZnO@MoS2 composites through hydrothermal and solvothermal method for photocatalytic hydrogen evolution. The structural, morphological, surface area and optical properties were investigated using transmission electron microscopy (HR-TEM), X-ray diffractometer (XRD), Brunauer Emmett Teller (BET), UV–visible (UV-vis) absorption and Photoluminescence (PL) emission spectroscopy. The incorporating effect of MoS2 on the photocatalytic performance of ZnO photocatalyst has been studied. The PL emission spectra of prepared composites elucidate that recombination of electron/hole pairs is greatly suppressed owing to the incorporation of MoS2 sheet-like nanostructures. The composite sample (3wt % of MoS2 in ZnO) showed the excellent photocatalytic efficiency when compared to pure photocatalyst. The considerable increase in the efficiency of nanocomposites may be accredited to extended absorption region, favorable band structure, and effective separation of charge carriers, large surface area and the reactive active sites provided by layered structure of MoS2. This study demonstrates that prepared composites could be promising and efficient photocatalysts for the evolution of hydrogen through water-splitting under visible light illumination.

Keywords $ZnO@MoS_2$ composite · H_2 evolution · Photocatalytic activity · Photocatalyst

Introduction

Clean and renewable energy is probably the most important challenge facing mankind in the twenty-first century. It is estimated that global energy demand doubled in the middle of this century, and by 2100, global energy demand will be tripled. One of the most important goals of our modern society is to build a sustainable environment (Gertler et al. 2019). The growing environmental problems associated with the widespread use of unsustainable fossil fuels (oil, natural gas and coal) and the growing demand for energy will sooner or later force humans to use clean and sustainable energy. Over the years, the scarcity of fossil fuels from biological remains of dead animals and plants for hundreds of millions of years ago and the environmental problems caused by their combustion have prompted research into the development of novel renewable energy production technique. Several methods have been proposed so far (Papadimitriou 2019; Tronchin et al. 2018). A combination of photocatalysts and solar energy has been identified by investigators as an associated source of clean and abundant energy (Christoforidis and Fornasiero 2017). The sun produces about 3×10^{24} J of energy each year, about 12,000 times greater than current energy requirement (Shaner 2016). Therefore, solar energy can be used as an alternative energy source. So far, water-splitting converts solar energy into hydrogen and considered an effective hydrogen preparation method to solve the energy problem. Research on photocatalysis has been carried out since last century and make a significant

✉ Muhammad Bilal Tahir
m.bilaltahir7@gmail.com

1 Department of Physics, HH Campus, University of Gujrat, Gujrat 50700, Pakistan

2 Department of Physics, University of Sahiwal, Sahiwal, Pakistan

3 Department of Chemical Engineering, HH Campus, University of Gujrat, Gujrat 50700, Pakistan

4 Department of Computer Science, HH Campus, University of Gujrat, Gujrat 50700, Pakistan

5 Research Center for Advanced Material Science (RCAMS), King Khalid University, 61413, Abha 9004, Saudi Arabia

6 Department of Physics, College of Science, King Khalid University, 61413, Abha 9004, Saudi Arabia

contribution to renewable energy and environmental treatment process (cleaning of emissions and purification of water). In the past decades, the number of applications based on photocatalysis has greatly increased. Although various material systems have been developed, the production of H_2 from water is one of the most promising ways to fulfil the current environmentally friendly energy demand (Sattler 2017; Hosseini and Wahid 2019; Rathod et al. 2016) because this technology is based on the energy of photons (or solar energy), which is a source of clean and permanent energy, mainly water, a renewable resource. It is an environmental protection technology, free of harmful by-products and pollutants. Using photocatalytic process, conversion of solar energy to hydrogen is a noble solution for energy and environmental problems (Chen et al. 2017). But the biggest challenge in using this technology is to develop high-quality and efficient photocatalyst which must have properties, such as higher electron–hole pair separation rate and higher surface-to-volume ratio for maximum interaction (Di 2016; Tan 2017; Sreethawong et al. 2008; Wang 2019). A huge effort has been made recently to build efficient photocatalytic systems, based on semiconductor materials photocatalyst, such as metal oxides (Kakuta and Abe 2009; Alkaim 2013), organic polymers (Jun 2013; Schwab 2010), sulfides (Xie et al. 2014), phosphates (Yi 2010), oxy-nitrides (Maeda et al. 2013), etc. Among all of these semiconductors, photocatalyst ZnO is a strong candidate for efficient photocatalyst because of its low cost, excellent stability, availability, and wide band gap and non-toxic properties. However, for H_2 evolution, pure ZnO shows weak photocatalytic activity. Rapid electron–hole pair recombination before migrating to the surface through the reaction is one of the reasons for non-effective photocatalyst for H_2 evolution (Pan and Zhang 2012; Kumar and Rao 2015). Loading noble metal on the surface of ZnO is an effective method to form ZnO metal hetero-structure to eliminate electron–hole recombination and increase photocatalysis ZnO efficiency. Many successful systems have been established to combine ZnO and various precious metals (such as Ag, Pt, and Au) to evolve H_2 (Gao et al. 2013; Chung 2019; He 2014). Due to the high cost of these precious noble metals, these are not suitable commercially as a photocatalyst. So, it is necessary for making highly efficient ZnO-based photocatalyst to explore co-catalysts which are easily available and low cost. MoS_2 is an exceptional photocatalyst for H_2 evolution in photocatalytic activity and also shows extensive applications toward a number of semiconductors, such as C_3N_4,(Hou 2013) CdSe (Frame and Osterloh 2010), $ZnIn_2S_4$ (Wei 2014) and TiO_2 (Zhou et al. 2013). Experimental and theoretical results also show that the active site of MoS_2 for the H_2 production reaction of unsaturated sulfur atoms terminates at the end of Mo edge (Hinnemann 2005; Sabbah 2007). A large number of studies have shown that the activity of MoS_2 is higher than from mostly used noble metal, such as Pb, Pt, Rh, Au and Pd (Sabbah 2007; Zong 2008). MoS_2 is not only suitable for (Hou 2013; Hinnemann 2005) electron–hole separation rate, but also provides favorable proton reduction sites in response to highly H_2 evolution reactions. Therefore, MoS_2 is considered the best co-catalyst for H_2 evolution and suitable alternative for noble metal because it is of less cost, outstanding photo-stability, easily available and non-toxic. ZnO is expected to hybridize with the MoS_2 layer, reduce electron–hole pair recombination rate and increase photocatalytic activity. Current research work focus on fabrication of ZnO–MoS_2 photocatalyst for hydrogen evolution. First, we synthesized pure ZnO and MoS_2 via hydrothermal and solvothermal method, respectively, and then combine both of these via hydrothermal method to study the effect of different concentration of MoS_2 in ZnO. Four composite samples of ZnO–MoS_2 are fabricated by varying MoS_2 (1–4%) concentration in pure ZnO.

Materials and methods

Fabrication of ZnO

To fabricate ZnO, 2 g of zinc acetate was dissolve in 80 ml ethanol. Then, NaOH solution was prepared in water separately and added drop-wise under constant stirring in zinc acetate solution until pH of the solution changed from 9 to 11 and maintained. Then, 80 ml solution was placed in sealed 100 ml Teflon autoclave and heated at 150^0C for 12 h. After reaction was complete, autoclaves were allowed to cool at room temperature. ZnO nanoparticles in white color were collected after filtering, and then washed with ethanol three to four times. To get good crystallinity, calcination of the sample was done at 500 °C for 2 h.

Fabrication of MoS_2

To fabricate MoS_2, as a starting material and source CH_4N_2S thioure, citric acid ($C_6H_6O_7$) and hepta-molybdate tetra-hydrate ($(NH_4)_6Mo_7O_{24}.4H_2O$) were used. Two solutions were prepared; in the first solution, 1.5 g of $(NH_4)_6Mo_7O_{24}.4H_2O$ with 0.5 g of $C_6H_6O_7$ was dissolved in distilled water under constant stirring at 85 °C for 30 min and during stirring, ammonia was added drop-wise until 4 pH of the solution was maintained. In the second solution, 1.30 g of CH_4N_2S was added drop-wise in distilled water under constant stirring on hot plate for 10 min. Then, both solutions were transferred to 100 ml Teflon autoclave and heated at 180 °C for 12 h. After reaction was complete, autoclaves were allowed to cool at room temperature. Black color precipitates were collected, then filtered and washed

with ethanol three to four times. To get good crystallinity, calcination of the sample was done at 400 °C for 2 h.

Assembling of ZnO–MoS_2 composite

Four samples (1–4) of composite ZnO–MoS_2 were prepared by varying the mass fraction of MoS_2 1%, 2%, 3% and 4% in pure ZnO sample by hydrothermal method. First, sample was prepared by taking 99wt % of ZnO mixed with 1wt % of MoS_2 for gelatinization and dispersion and added in deionized water. Then, sample was centrifuged at 3000 rpm for 40 min and dried at 200 °C on magnetic stirrer. Similarly, second, third and fourth samples were prepared by varying 2wt %, 3wt % and 4wt % of MoS_2 in pure ZnO particles.

Characterization

Morphology and composition of the synthesized samples were determine by TEM (JEM-2100). Optical and electronic properties of fabricated samples were investigated by UV–visible spectroscopy (UV-1700, Shimadzu) and PL (FP-8200, JASCO), where the BET surface area of fabricated particles were determined using nitrogen (N_2) absorption device Micrometer TriStarII-3020 (Fig. 1).

Photocatalytic hydrogen production measurements

Green approach of H_2 production as a fuel is carried out in closed quartz reactor, and the reaction chamber was totally sealed so that no other gas exchange takes place in it. In the reaction chamber, 60 mg photocatalyst was used in 100 ml solution containing deionized water with 0.1 M Na_2S and 0.05 Na_2SO_3. 300-W Xeon Lamp was used as a light source for photocatalytic reaction with wavelength $\lambda \geq 400$ nm. Initially, reaction chamber was placed in the dark with constant stirring for 50 min and then to make homogenous solution treated ultrasonically for 10 min, after this, N_2 gas was used to exhaust O_2 from the reactor. Finally, reactor was exposed to light for H_2 evaluation. In reaction chamber, H_2 evaluation was examined by GC-7890II chromatograph (Ar carrier, *MS* − 5Å column, Beifen-Ruili, TCD and SP-2100).

Results and discussion

Photoluminescence (PL) spectrum is used to examine migration, electron–hole transfer efficiency and trapping in the semiconductors. PL spectra of pure ZnO and composite samples 1–4 were shown in (Fig. 2). PL spectra consist of two emission regions, one is UV region consisting of band-gap peaks that range 350–400 nm and the second one is general broad-band spectrum region inferring about the structural defect in fabricated samples that range 400–700 nm(Peng 2008; Park 2003). First, peaks of all samples observed in UV region almost at the same point show that because of minute doping variation in band-gap being very small. Other peaks are in visible region from 400 to 470 nm range and show the lattice defect in fabricated samples. Figure 2 depicts PL spectra, intensity peak falls down as compared to pure ZnO in composite samples, maximum intensity peak falls in sample three, high-intensity peak shows high electron–hole pair recombination, fall-down intensity peak representing electron–hole pair recombination decreases and suitable for photocatalytic reaction(Dong 2019; Li 2018). However, in sample 4, intensity peak once again rises by increasing the concentration of MoS_2 representing that further doping MoS_2 is not suitable as a photocatalyst.

UV–visible absorption spectra of pure ZnO and composite samples one and two are shown in Fig. 3.

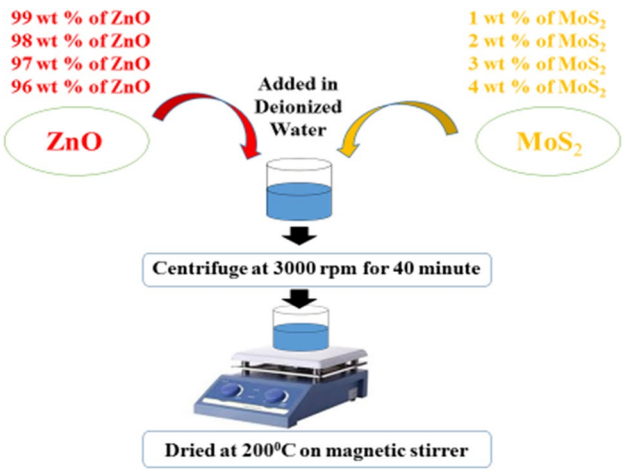

Fig. 1 Assembling of ZnO-MoS2 composite

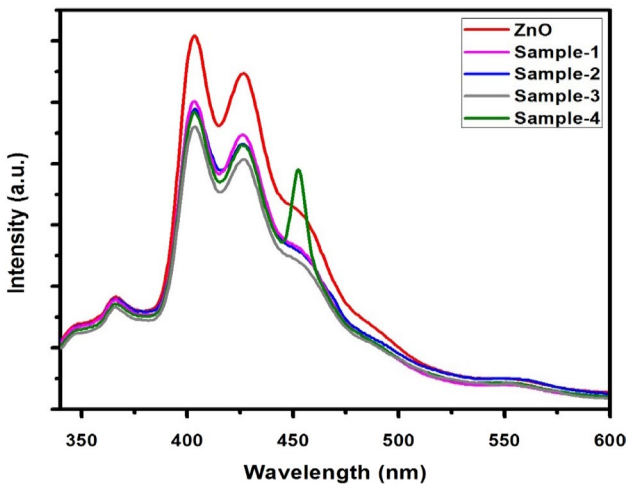

Fig. 2 Photoluminescence (PL) spectra of pure-ZnO composites (ZnO-MoS_2) samples

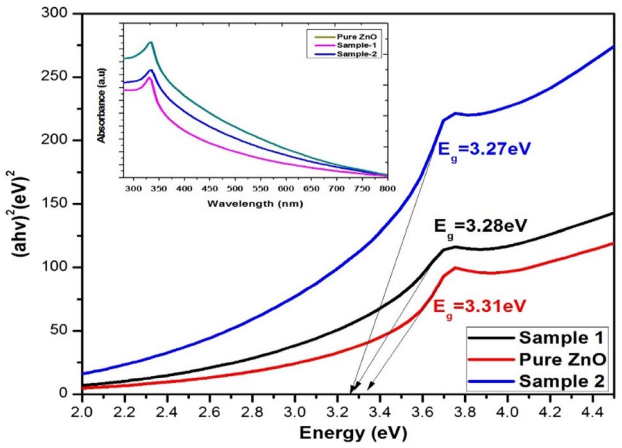

Fig. 3 UV–visible absorption spectra of pure-ZnO composites (ZnO-MoS_2) samples

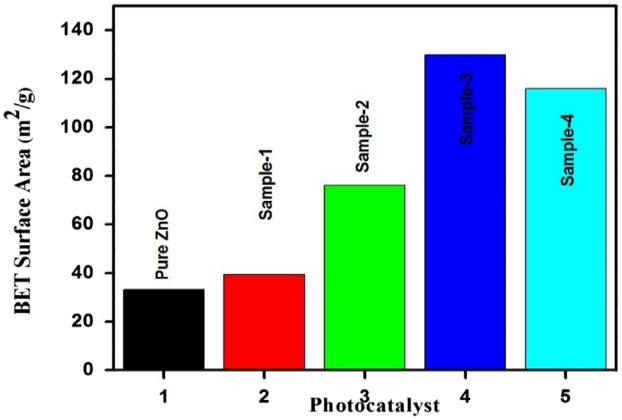

Fig. 4 BET-Surface area of pure-ZnO composites (ZnO-MoS_2) samples

Absorption peak of all three samples are observed in almost same range from 340 to 370 nm, which confirms, from doping of MoS_2 in the very minute of variation in band gap, that the same trend is observed in above PL spectra. Using Tauc plot relation, band gap of pure ZnO and composites sample were determine using relation describe in Eq. 1 (Saravanan 2016). In (Fig. 3), graph was plotted between energy versus α hv.

$$\alpha hv = K(hv - E_g)^n \quad (1)$$

Band gap of pure ZnO and composite samples are 3.31, 3.28 and 3.27, respectively. By varying the concentration of MoS_2, the band decreases toward the visible region because of very small doping minute variation observed like PL spectra but variation toward the visible region suitable for photocatalytic reaction (Nayak et al. 2015; Takanabe and Domen 2011).

BET surface area of pure ZnO and composite (ZnO–MoS_2) samples 1, 2, 3 and 4 are investigated via nitrogen absorption–desorption spectra shown in (Fig. 4). Results show that pure ZnO particles have surface area 33.19 m^2/g less than the ZnO–MoS_2 composite sample, as graphs in (Fig. 4) indicate, by increasing the concentration of MoS_2 in pure ZnO particle, surface area increased 39.43 m^2/g, 76.23 m^2/g and 129.79 m^2/g, respectively, suitable for effective photocatalyst (Tahir 2018). In the last sample, by further increasing the concentration 4wt % of MoS_2 in pure ZnO, surface area decreased 116.02 m^2/g as compared to sample 3. Same trend was also observed in TEM characterization pictures shown in (Fig. 5). By increasing the concentration in composite samples, particle size decreases as shown in (Fig. 5). 2-D clear nano-sheet morphology was observed in sample 3 that by further increasing the concentration of MoS_2 in sample 4, size increased and morphology scattered.

Photocatalytic activity for H_2 evolution with pure ZnO, MoS_2 and with composite (ZnO–MoS_2) samples 1–4 were shown in (Fig. 5). Minimum catalytic efficiency 15 $\mu molh^{-1}\ g^{-1}$ was observed from pure MoS_2, then catalytic efficiency varied with pure ZnO 29 $\mu molh^{-1}\ g^{-1}$ but not enough as an efficient photocatalyst. H_2 evolution results from composite (ZnO–MoS_2) as compared to pure samples remarkably, maximum H_2 evolution 165 $\mu molh^{-1}\ g^{-1}$ obtained from sample 3 (ZnO mixed with 3wt % of MoS_2), by varying the concentration of MoS_2 in pure-ZnO 1%, 2% and 3%. H_2 evolution efficiency increased 54 $\mu molh^{-1}\ g^{-1}$, 117 $\mu molh^{-1}\ g^{-1}$ and 165 $\mu molh^{-1}\ g^{-1}$, respectively, but in sample 4 (ZnO mixed with 4wt % of MoS_2), further increase in concentration causes decrease in H_2 evolution 141 $\mu molh^{-1}\ g^{-1}$ as compared to sample 3.

Here, different factors play an important role in H_2 evolution for efficient photocatalyst surface-to-volume ratio and morphology have an important role as also observed here in this photocatalytic activity. In (Fig. 4), BET surface area graph shows that pure ZnO has the smallest surface-to-volume ratio, and sample 3 has the highest surface-to-volume ratio, and then sample 4 surface-to-volume ratio decreases. Surface-to-volume ratio directly links with particle size. Similarly, in Fig. 5, TEM images show pure MoS_2 has the maximum size 50 µm and composite sample 3 has the smallest size 10 nm. So, according to TEM and BET surface, characterization in composite sample by varying the concertation of MoS_2 in samples 1–3 size decreases and surface-to-volume ratio increases and in sample 4, size once again increases and surface-to-volume ratio decreases. Overall, H_2 evaluation results are also according to the same trend and photocatalytic efficiency also directly links with surface-to-volume ratio. When high surface-to-volume ratio and maximum photo-catalytic surface are available for reaction, better results are obtained (Fig. 6).

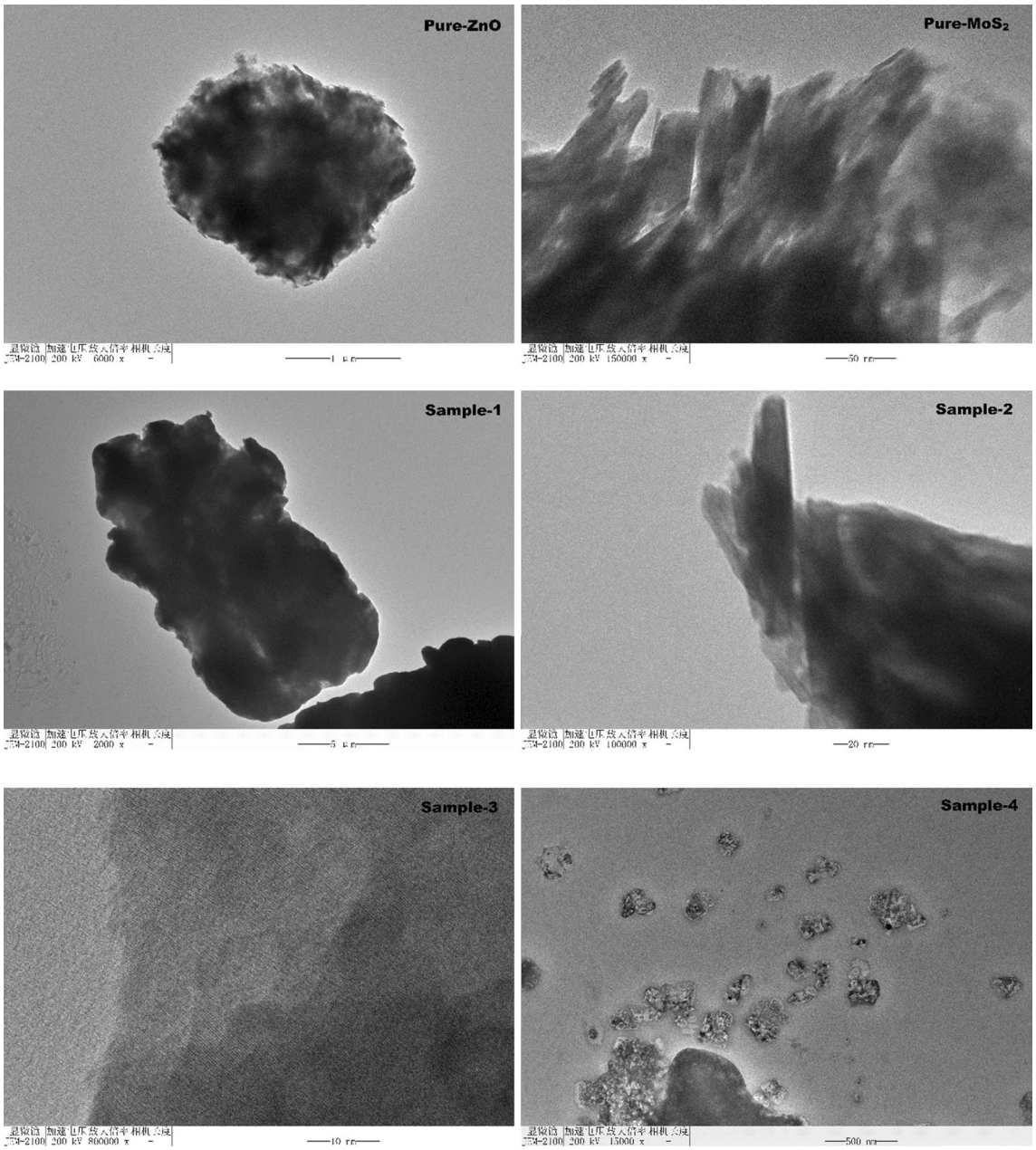

Fig. 5 TEM images of fabricated samples

Moreover, electron–hole pair recombination has an important role, weak activity of pure ZnO could be attributed to the rapid electron–hole pair recombination. MoS_2 loading on the pure ZnO surface caused a significant increase in H_2 production. Due to narrow band gap MoS_2, MoS_2 in composite ZnO–MoS_2 acts as photo-sensitizer like macro-molecule organic dye (Feng 2014). In addition, pure ZnO, after sensitization, effectively used visible light (Pawar and Lee 2014; Bu 2013). ZnO–MoS_2 intermediate contact and due to charge-carrier density at boundary, hole in MoS_2 diffuses in ZnO. Similarly, electron in pure ZnO diffuses to the MoS_2 and form positive- and negative-charged regions. These charged regions are the source of intermediate electrostatic field and band bending shown in (Fig. 7). Due to electrostatic field, photo-excited electron in MoS_2 conduction band transfers to ZnO and hole in ZnO transfers to the MoS_2. In this way, in composite ZnO–MoS_2, electron–hole pair separation rate increases and causes maximum H_2 evolution (Tan 2014; Tajima 1990). H_2 evolution activity of the photocatalyst loaded with a relatively high amount of MoS_2 (4wt % of MoS_2 in pure ZnO) can be attributed to the shading effect of MoS_2

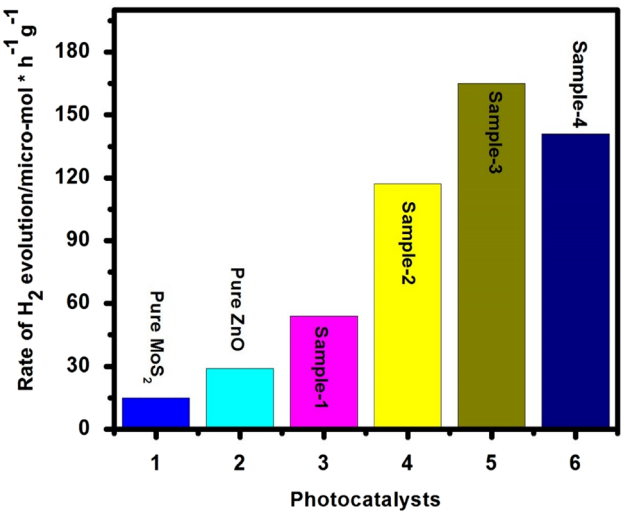

Fig. 6 Photocatalytic activity for H_2 evolution

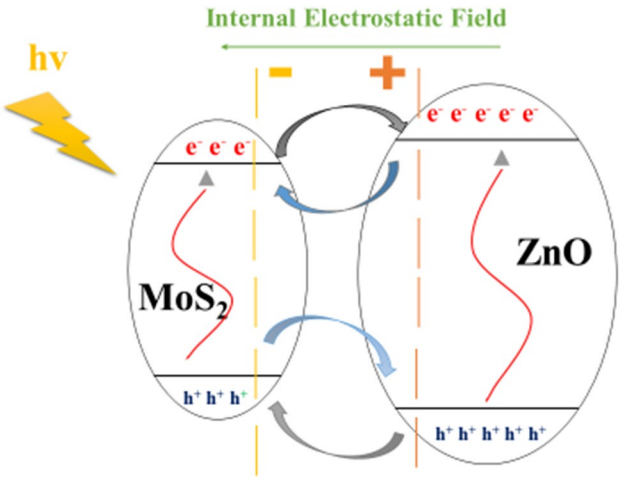

Fig. 7 Schematic diagram of electron hole pair separation due to internal electrostatic field

(Yuan 2015), which suppresses the easy absorption of light in ZnO component.

Conclusion

ZnO and MoS_2 samples were successfully fabricated via hydrothermal and solvothermal method, respectively, and ZnO-MoS_2 composite with different concentration of MoS_2 combined via hydrothermal method. For H_2 evolution, concentration of MoS_2 in composite samples (ZnO-MoS_2) plays an important role. In composite samples, varying concentration of MoS_2 directly affect the composite size, surface-to-volume ratio, electron–hole pair recombination rate and H_2 evolution activity. Maximum photocatalytic activity for H_2 evolution was observed with composite (3wt % of MoS_2 in pure ZnO). Further increase in concentration may cause to lower the photocatalytic performance owing to surface-to-volume ratio and electron–hole pair recombination rate.

Acknowledgments The authors from the King Khalid University, Saudi Arabia acknowledge the financial and technical support from Research Center for Advanced Material Science (RCAMS) at King Khalid University through grant number RCAMS/KKU/014–20.

Compliance with ethical standards

Conflict of interest The authors declare that there is no conflict of interest.

References

Alkaim AF et al (2013) Solvent-free hydrothermal synthesis of anatase TiO2 nanoparticles with enhanced photocatalytic hydrogen production activity. Appl Catal A 466:32–37

Bu Y et al (2013) Highly efficient photocatalytic performance of graphene–ZnO quasi-shell–core composite material. ACS Appl Mater Int 5(23):12361–12368

Chen S, Takata T, Domen K (2017) Particulate photocatalysts for overall water splitting. Nat Reviews Mater 2(10):1–17

Christoforidis KC, Fornasiero P (2017) Photocatalytic hydrogen production: a rift into the future energy supply. ChemCatChem 9(9):1523–1544

Chung W-C et al (2019) Removal of VOCs from gas streams via plasma and catalysis. Catalysis Rev 61(2):270–331

Di T et al (2016) Enhanced photocatalytic H2 production on CdS nanorod using cobalt-phosphate as oxidation cocatalyst. Appl Surf Sci 389:775–782

Dong H et al (2019) High-throughput production of ZnO-MoS2-graphene heterostructures for highly efficient photocatalytic hydrogen evolution. Materials 12(14):2233

Feng Y et al (2014) An in situ gelatin-assisted hydrothermal synthesis of ZnO–reduced graphene oxide composites with enhanced photocatalytic performance under ultraviolet and visible light. RSC Adv 4(16):7933–7943

Frame FA, Osterloh FE (2010) CdSe-MoS2: a quantum size-confined photocatalyst for hydrogen evolution from water under visible light. J Phys Chem 114(23):10628–10633

Gao P, Liu Z, Sun DD (2013) The synergetic effect of sulfonated graphene and silver as co-catalysts for highly efficient photocatalytic hydrogen production of ZnO nanorods. J Mater Chem 1(45):14262–14269

Gertler P et al (2016) (2019) Replication data for: the demand for energy-using assets among the world's rising middle classes. Am Eco Rev 106(6):1366–1401

He L et al (2014) Fabrication of Au/ZnO nanoparticles derived from ZIF-8 with visible light photocatalytic hydrogen production and degradation dye activities. Dalton Trans 43(45):16981–16985

Hinnemann B et al (2005) Biomimetic hydrogen evolution: MoS2 nanoparticles as catalyst for hydrogen evolution. J Am Chem Soc 127(15):5308–5309

Hosseini SE, Wahid MA (2019) Hydrogen from solar energy, a clean energy carrier from a sustainable source of energy. Intern J Energy Res 1:1

Hou Y et al (2013) Layered nanojunctions for hydrogen-evolution catalysis. Angew Chem Int Ed 52(13):3621–3625

Jun YS et al (2013) From melamine-cyanuric acid supramolecular aggregates to carbon nitride hollow spheres. Adv Func Mater 23(29):3661–3667

Kakuta S, Abe T (2009) A novel example of molecular hydrogen generation from formic acid at visible-light-responsive photocatalyst. ACS Appl Mater Interfaces 1(12):2707–2710

Kumar SG, Rao KK (2015) Zinc oxide based photocatalysis: tailoring surface-bulk structure and related interfacial charge carrier dynamics for better environmental applications. Rsc Advances 5(5):3306–3351

Li H et al (2018) Enhanced photocatalytic activity and synthesis of ZnO nanorods/MoS2 composites. Superlattices Microstruct 117:336–341

Maeda K, Lu D, Domen K (2013) Direct water splitting into hydrogen and oxygen under visible light by using modified TaON photocatalysts with d0 electronic configuration. Chem European J 19(16):4986–4991

Nayak S, Mohapatra L, Parida K (2015) Visible light-driven novel gC 3 N 4/NiFe-LDH composite photocatalyst with enhanced photocatalytic activity towards water oxidation and reduction reaction. J Mater Chem 3(36):18622–18635

Pan H, Zhang Y-W (2012) GaN/ZnO superlattice nanowires as photocatalyst for hydrogen generation: a first-principles study on electronic and magnetic properties. Nano Energy 1(3):488–493

Papadimitriou C et al (2019) Demand response schemes in energy hubs: a comparison study. Energy Procedia 157:939–944

Park WI et al (2003) Excitonic emissions observed in ZnO single crystal nanorods. Appl Phys Lett 82(6):964–966

Pawar RC, Lee CS (2014) Single-step sensitization of reduced graphene oxide sheets and CdS nanoparticles on ZnO nanorods as visible-light photocatalysts. Appl Catal B 144:57–65

Peng X et al (2008) Structural and PL properties of Cu-doped ZnO films. J Lumin 128(3):297–300

Rathod VP, Shete J, Bhale PV (2016) Experimental investigation on biogas reforming to hydrogen rich syngas production using solar energy. Int J Hydrogen Energy 41(1):132–138

Sabbah H et al (2007) SJ 70 Klippenstein and IWM Smith. Science 317:100–102

Saravanan R et al (2016) Conducting PANI stimulated ZnO system for visible light photocatalytic degradation of coloured dyes. J Mol Liq 221:1029–1033

Sattler C et al (2017) Solar hydrogen production via sulphur based thermochemical water-splitting. Sol Energy 156:30–47

Schwab MG et al (2010) Photocatalytic hydrogen evolution through fully conjugated poly (azomethine) networks. Chem Commun 46(47):8932–8934

Shaner MR et al (2016) A comparative technoeconomic analysis of renewable hydrogen production using solar energy. Energy Environ Sci 9(7):2354–2371

Sreethawong T, Laehsalee S, Chavadej S (2008) Comparative investigation of mesoporous-and non-mesoporous-assembled TiO2 nanocrystals for photocatalytic H2 production over N-doped TiO2 under visible light irradiation. Int J Hydrogen Energy 33(21):5947–5957

Tahir MB (2018) Construction of MoS 2/CND-WO 3 ternary composite for photocatalytic hydrogen evolution. J Inorg Organomet Polym Mater 28(5):2160–2168

Tajima H et al (1990) Utilization of MOS gate structure for capacitive charge division readout of silicon strip detector. Nucl Instrum Methods Phys Res 288(2–3):536–540

Takanabe K, Domen K (2011) Toward visible light response: overall water splitting using heterogeneous photocatalysts. Green 1(5–6):313–322

Tan Y-H et al (2014) MoS2@ ZnO nano-heterojunctions with enhanced photocatalysis and field emission properties. J Appl Phys 116(6):064305

Tan Y et al (2017) Charge-compensated (Nb, Fe)-codoped La2Ti2O7 photocatalyst for photocatalytic H2 production and optical absorption. J Alloy Compd 709:277–284

Tronchin L, Manfren M, Nastasi B (2018) Energy efficiency, demand side management and energy storage technologies–a critical analysis of possible paths of integration in the built environment. Renew Sust Energy Rev 95:341–353

Wang S et al (2019) Direct Z-scheme ZnO/CdS hierarchical photocatalyst for enhanced photocatalytic H2-production activity. Appl Catal B 243:19–26

Wei L et al (2014) MoS2 as non-noble-metal co-catalyst for photocatalytic hydrogen evolution over hexagonal ZnIn2S4 under visible light irradiations. Appl Catal B 144:521–527

Xie Y et al (2014) Role of surface structure on Li-ion energy storage capacity of two-dimensional transition-metal carbides. J Am Chem Soc 136(17):6385–6394

Yi Z, Ye J, Kikugawa N, Kako T, Ouyang S, Stuart-Williams H, Yang H, Cao J, Luo W, Li Z, Liu Y (2010) An orthophosphate semiconductor with photooxidation properties under visible-light irradiation. Nat Mater 9(7):559–564

Yuan Y-J et al (2015) Significant enhancement in photocatalytic hydrogen evolution from water using a MoS2 nanosheet-coated ZnO heterostructure photocatalyst. Dalton Trans 44(24):10997–11003

Zhou W et al (2013) Synthesis of few-layer MoS2 nanosheet-coated TiO2 nanobelt heterostructures for enhanced photocatalytic activities. Small 9(1):140–147

Zong X et al (2008) Enhancement of photocatalytic H2 evolution on CdS by loading MoS2 as cocatalyst under visible light irradiation. J Am Chem Soc 130(23):7176–7177